

Self-organized vascular networks from human pluripotent stem cells in a synthetic matrix

Sravanti Kusuma^{a,b}, Yu-I Shen^a, Donny Hanjaya-Putra^a, Prashant Mali^{b,c,1}, Linzhao Cheng^c, and Sharon Gerecht^{a,d,2}

^aDepartment of Chemical and Biomolecular Engineering, Johns Hopkins Physical Sciences–Oncology Center and Institute for NanoBioTechnology, and ^bDepartment of Biomedical Engineering, Johns Hopkins University, Baltimore, MD 21218; ^cInstitute for Cell Engineering and Division of Hematology, Johns Hopkins School of Medicine, Baltimore, MD 21287; and ^dDepartment of Materials Science and Engineering, Johns Hopkins University, Baltimore, MD 21218

Edited by Robert Langer, Massachusetts Institute of Technology, Cambridge, MA, and approved June 14, 2013 (received for review April 7, 2013)

The success of tissue regenerative therapies is contingent on functional and multicellular vasculature within the redeveloping tissue. Although endothelial cells (ECs), which compose the vasculature's inner lining, are intrinsically able to form nascent networks, these structures regress without the recruitment of pericytes, supporting cells that surround microvessel endothelium. Reconstruction of typical in vivo microvascular architecture traditionally has been done using distinct cell sources of ECs and pericytes within naturally occurring matrices; however, the limited sources of clinically relevant human cells and the inherent chemical and physical properties of natural materials hamper the translational potential of these approaches. Here we derived a bicellular vascular population from human pluripotent stem cells (hPSCs) that undergoes morphogenesis and assembly in a synthetic matrix. We found that hPSCs can be induced to codifferentiate into early vascular cells (EVCs) in a clinically relevant strategy amenable to multiple hPSC lines. These EVCs can mature into ECs and pericytes, and can self-organize to form microvascular networks in an engineered matrix. These engineered human vascular networks survive implantation, integrate with the host vasculature, and establish blood flow. This integrated approach, in which a derived bicellular population is exploited for its intrinsic self-assembly capability to create microvasculature in a deliverable matrix, has vast ramifications for vascular construction and regenerative medicine.

codifferentiation | hydrogels

Perhaps the greatest roadblock to the success of tissue regenerative therapies is the establishment of a functional microvascular network to support tissue survival and growth (1). Microvascular construction or regeneration depends on endothelial morphogenesis into a 3D tubular network, followed by stabilization of the assembling structures by recruited pericytes (2, 3). To create such a construct for therapeutic applications, patient-derived ECs and pericytes must be incorporated into a synthetic matrix, which confers an advantage in controlling and modulating vascular morphogenesis and also represents a clinically relevant construct in which to deliver the engineered microvascular networks to in vivo environments (4).

Human pluripotent stem cells (hPSCs), including human embryonic stem cells (hESCs) and human induced PSCs (hiPSCs), offer the opportunity to derive EVCs from the same source, which offers patient specificity. Various cell markers have been proposed to identify vascular precursors (of ECs and pericytes) from differentiating hPSCs including CD34 (5, 6), VEGF receptor-2 (VEGFR2)/kinase domain receptor (KDR) (7), and apelin receptor (8). Purification of such progenitors is required from an uncontrolled differentiated cell population [i.e., via embryoid body (EB) formation or coculture on mouse feeder layer] through marker enrichment or selection through genetic manipulation. Importantly, none of these derived cells have been demonstrated to self-assemble into functional microvasculature containing both ECs and pericytes.

Current approaches for the differentiation of hPSCs toward the vascular lineage typically use a purified, single derivative—either

a progenitor or a mature cell type—with the goal of fully characterizing the fidelity of differentiation from a PSC. From this body of work, it has become apparent that various cell markers and biochemical cues can be used to guide differentiation and derive functional ECs (5, 9–12), vascular smooth muscle cells (5, 11, 13) and pericytes (14). Building on these previous studies, in the present study we hypothesized that hPSCs can be induced to differentiate into early derivatives of the vascular lineage (i.e., EVCs) that compose the microvascular architecture without a specific differentiation-inducible feeder layer, EB formation, or genetic manipulation (Fig. 1*A*, *i*); and that such EVCs can mature into ECs and pericytes and can self-assemble to form vascular networks in an engineered matrix (Fig. 1*A*, *ii*).

We present a unique conceptual approach in which the cells of the microvasculature are derived in a bipotent population, which is able to recreate the tissue. Our protocol uses a monolayer culture and avoids an EB intermediate and sorting, thereby enabling reproducibility and clinical applicability. We harness intrinsic tissue-level differentiation and self-assembly capabilities toward the translational realization of hPSCs. This paradigm could prove useful for the construction of other multicellular tissues for regeneration.

Results and Discussion

Derivation of EVCs from hPSCs. Toward clinically relevant outcomes, and because microvascular architecture is a bicellular entity, we first sought to develop a robust and controlled method to differentiate hPSCs into a bicellular vasculogenic population with maturation capacity to both ECs and pericytes. CD105 and CD146 are common to both cell types (14–17), whereas vascular endothelial cadherin (VEcad) has been shown to specify a lineage commitment of ECs (10). Although no single marker designates pericytes, pericytes can be distinguished by the expression of platelet-derived growth factor β (PDGFR β) in conjunction with CD146 (18).

Acknowledging that cocultures of pericytes and ECs typically result in pericyte-mediated EC growth inhibition (14, 19), we focused on inducing VEcad⁺ cells early in the differentiation process to ensure EC maturation. Building on previous work (10, 20, 21), we developed a stepwise differentiation procedure to induce vascular lineage specification. hPSCs (*SI Appendix*, Table S1) were first allowed to undergo differentiation in a monolayer (*SI Appendix*, Fig. S1). The subsequent addition of TGF- β inhibitor SB431542 (10), supplemented with either high (50 ng/mL) or low (1 ng/mL) concentrations of VEGF-A yielded up-

Author contributions: S.K. and S.G. designed research; S.K., Y.-I.S., and D.H.-P. performed research; Y.-I.S., D.H.-P., P.M., and L.C. contributed new reagents/analytic tools; S.K., Y.-I.S., D.H.-P., and S.G. analyzed data; and S.K., L.C., and S.G. wrote the paper.

The authors declare no conflict of interest.

This article is a PNAS Direct Submission.

¹Present address: Department of Genetics, Harvard Medical School, Boston, MA 02115.

²To whom correspondence should be addressed. E-mail: gerecht@jhu.edu.

This article contains supporting information online at www.pnas.org/lookup/suppl/doi:10.1073/pnas.1306562110/-DCSupplemental.

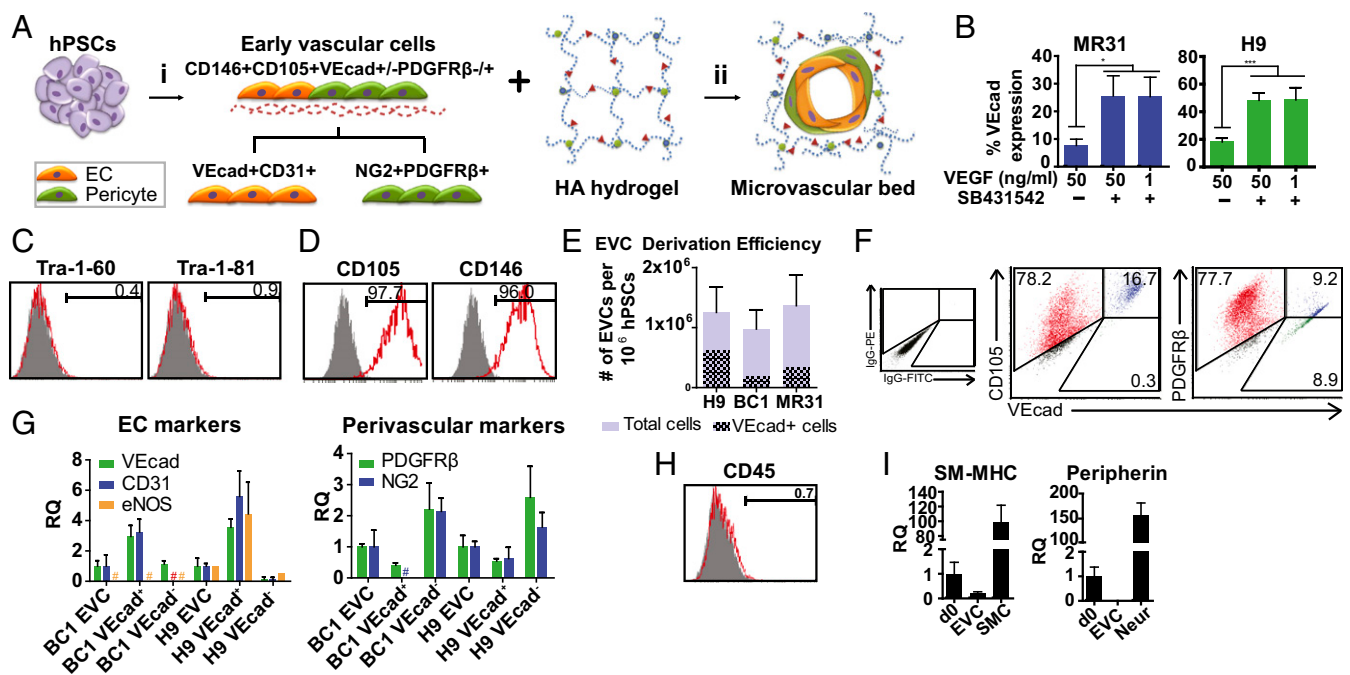


Fig. 1. Derivation of EVCs from hPSCs. (A) Schema for self-assembled vascular derivatives. (i) hPSCs are differentiated toward EVCs that can be matured into functional ECs and pericytes. (ii) Derived EVCs are embedded within a synthetic HA matrix that facilitates self-organization into vascular networks. (B) VEcad expression in day 12 differentiated hiPSC-MR31 and hESC-H9 cell lines comparing the three differentiation conditions tested (flow cytometry analysis; $n = 3$). (C and D) Flow cytometry plots ($n = 3$) of EVC derivatives assessing the expression of pluripotency markers TRA-1-60 and TRA-1-81 (C) and CD105 and CD146 (D). (E) EVC differentiation efficiency from hPSC lines per 1 million input hPSCs. (F) Flow cytometry plots ($n = 3$) of EVC derivatives assessing expression of VEcad double-labeled with CD105 or PDGFR β . (Left) Isotype controls. (G) Quantitative RT-PCR analysis of EC and perivascular marker expression by EVCs and sorted VEcad⁺ and VEcad⁻ cells. # denotes not detected. Data are normalized to EVCs of each specific hPSC type. (H) Flow cytometry plots ($n = 3$) of hematopoietic marker CD45 (hiPSC-BC1). (I) Quantitative RT-PCR of H9-EVCs for the expression of SMMHC and peripherin, compared with undifferentiated cells (d0) and mature derivatives (13, 37). Isotype controls for flow cytometry are in gray. Flow cytometry results shown are typical of the independent experiments. * $P < 0.05$; ** $P < 0.01$; *** $P < 0.001$.

regulation of VEcad expression ranging from 20% to 60% VEcad⁺ cells, depending on hPSC line (Fig. 1B and *SI Appendix, Fig. S2*).

Under our differentiation strategy, hESC line H9 exhibited the greatest potential to yield the largest percentage of VEcad⁺ cells compared with hiPSC lines BC1 and MR31. The expression levels of CD31 were not changed under the various conditions, whereas VEGFR2/KDR expression was higher in media supplemented with a low VEGF concentration (*SI Appendix, Fig. S3*). Expression of tumor rejection antigen (TRA)-1-60 and TRA-1-81, markers of pluripotency, was <1% when using high VEGF concentrations, indicating that the vast majority of cells had been differentiated (Fig. 1C and *SI Appendix, Fig. S3*). Thus, in all experiments, EVCs were differentiated in medium supplemented with SB431542 and with high VEGF concentrations.

EVCs derived from multiple hPSC lines using high VEGF concentrations and SB431542 were highly purified (>95%) for CD105 and CD146, surface antigens common to both ECs and pericytes (Fig. 1D and *SI Appendix, Fig. S4 A–C*), expanding on a previously reported approach that sorted out a CD105⁺ population from spontaneously differentiating EBs with the focus on pericytes (14). By eliminating a sorting step and guiding hPSCs toward a bipotent population, our approach builds on this previous study and provides a unique strategy to yield a CD105⁺ CD146⁺ population that composes the bicellular microvascular architecture in a controlled, efficient, and robust manner.

Without our specific inductive protocol (i.e., removal of VEGF and SB431542 supplementation), hiPSC-BC1 cells differentiated for 12 d were still fairly well enriched in CD105 (95%) and CD146 (93%); however, hESC-H9 cells differentiated for 12 d

without these inductive conditions expressed ~90% CD105⁺ cells and only 54% CD146⁺ cells (*SI Appendix, Fig. S4D*). Importantly, both H9 and BC1 differentiated cell populations expressed very low levels of VEcad. These results, along with the aforementioned finding that high VEGF supplementation ensures <1% TRA-1-60⁺ cells in the various hPSC types (Fig. 1C and *SI Appendix, Fig. S3*), further support our choice of inductive media conditions.

Using our approach, we derived CD105⁺CD146⁺ EVCs at an approximate ratio of 1:1 of input hPSC to EVC (Fig. 1E). The number of input hPSCs was calculated as the number seeded at day 0, not the number of cells present after 1 d of differentiation, as reported previously (10). The yield of VEcad⁺ cells in EVCs varied among cell lines, ranging from $\sim 8 \times 10^4$ to 2.5×10^5 per 10⁶ hPSCs (Fig. 1E), similar to what has been recently reported for KDR⁺ EC derivatives (22). Flow cytometry analysis of EVCs double-labeled with antibodies against CD105 and VEcad confirmed that a subset of cells coexpressed CD105 and VEcad (Fig. 1F, Left). In contrast, EVCs double-labeled for VEcad and PDGFR β revealed two distinct VEcad⁺PDGFR β ^{lo} and VEcad⁺PDGFR β ⁺ populations (Fig. 1F, Right and *SI Appendix, Fig. S5*).

RT-PCR analysis of sorted VEcad⁺ and VEcad⁻ subpopulations from EVCs revealed distinct phenotypes (Fig. 1G). VEcad⁺ cells from both hESC-H9 and hiPSC-BC1 cell lines demonstrated greater expression of EC markers VEcad and CD31 compared with unsorted EVCs and sorted VEcad⁻ subpopulations. Of note, endothelial nitric oxide synthase (eNOS), a mature EC marker, was highly expressed in H9-VEcad⁺ cells compared with H9 EVCs and sorted VEcad⁻ cells, whereas

eNOS was undetected in all tested BC1 samples. Sorted VECad⁻ cells exhibited greater expression of pericyte markers PDGFR β and NG2 compared with EVCs and sorted VECad⁺ cells.

Our analysis also revealed differences in the differentiation potential between hESC-H9 and hiPSC-BC1 lines using the adherent, stepwise differentiation protocol, suggesting that hESC-H9-differentiating cells may mature more rapidly toward these lineages, owing to the fact that 12-d differentiated H9-EVCs started to express eNOS at the mRNA level and yielded a greater percentage of VECad⁺ (Fig. 1B) and CD31⁺ cells at the protein level (SI Appendix, Fig. S3) compared with the tested hiPSC lines.

EVCs were negative for hematopoietic marker CD45 (Fig. 1H), and demonstrated negligible expression of the smooth muscle cell marker smooth muscle myosin heavy chain (SMMHC), as well as the peripheral neuron marker peripherin (Fig. 1I). Comparable marker expression profiles were obtained from EVCs derived using serum-free conditions in our adherent differentiation scheme (SI Appendix, Fig. S6). Based on these analyses, we considered this derived population to be vascular lineage-specific and composed of early ECs and early pericytes. It should be noted that these are not mature ECs and pericytes, given that 12 d of differentiation was not sufficient to mature hPSCs toward matured phenotypes, in agreement with numerous previous studies (5, 14, 23).

Maturation of EVCs: ECs. We took two approaches to examine the endothelial potential of hPSC-EVCs, (i) subculturing EVCs and (ii) sorting and expanding VECad⁺ cells, both under the same culture conditions (i.e., 50 ng/mL VEGF and SB431542). Subculturing yielded ECs that were enriched in VECad and CD31 (SI Appendix, Fig. S7 A and B); however, this approach and enrichment without cell sorting varied among three different hPSC lines, and a hiPSC line with vector integration demonstrated the best results (SI Appendix, Fig. S7C). Sorted VECad⁺ cells from EVCs matured toward VECad⁺CD31⁺CD146⁺ ECs (Fig. 2A). The cells exhibited typical membrane expression of VECad and CD31, lectin binding, cytoplasmic expression of eNOS and von Willebrand factor (vWF), uptake of acetylated low-density lipoprotein (acLDL), up-regulation of intercellular adhesion molecule 1 (ICAM1) in response to TNF- α , and network formation on Matrigel (Fig. 2B and SI Appendix, Fig. S7 D and E). We did not detect lectin, eNOS, vWF, or acLDL uptake via immunofluorescence in our unsorted EVC populations,

demonstrating that no subpopulation of EVCs expresses these EC characteristics and that additional culture is needed to mature early ECs from EVCs. These findings were consistent among the different hPSC lines examined.

Maturation of EVCs: Pericytes. We next probed the pericyte potential of the EVCs. EVCs, which do not express NG2 (SI Appendix, Fig. S8A), were cultured under pericyte-inducing conditions (19). After 6 d of culture, cells were enriched in pericyte markers CD73, NG2, PDGFR β , and CD44 (24) and depleted in EC markers VECad and CD31 (Fig. 2C and SI Appendix, Fig. S8A). Interestingly, most cells retained CD146⁺ expression, but some lost CD105 expression (Fig. 2C). The spindle-shaped pericyte derivatives expressed PDGFR β and NG2 proteoglycan and exhibited filamentous calponin expression (Fig. 2D), as would be expected for pericytes derived from fetal and adult sources. Sorted VECad⁺ cells were not able to attach and grow under pericyte-maturing conditions. An important function of pericytes is their ability to behave as mesenchymal precursors (14, 18). Indeed, the pericyte derivatives in our culture could be differentiated to adipocytes and osteoblasts (SI Appendix, Fig. S8 B and C), demonstrating their mesenchymal potential.

Furthermore, sorted VECad⁻ cells, cultured under either EC maturation conditions (50 ng/mL VEGF and SB431542) or pericyte-maturing conditions for 6 d, expressed NG2, PDGFR β , and CD44 (SI Appendix, Fig. S9). A small population (~8%) of sorted VECad⁻ cells acquired VECad expression (but not CD31 expression) when cultured under EC maturation conditions, indicating some degree of cellular plasticity.

Taken together, our cellular analysis results demonstrate that EVCs composed of CD105⁺CD146⁺VECad⁺ and CD105⁺CD146⁺PDGFR β ⁺ subtypes contain the cellular makeup necessary for constructing a microvasculature.

Self-Organization of Bicellular Vascular Networks in Hydrogels. To examine whether EVCs could be leveraged to self-organize into a bicellular microvascular bed, we tested network formation in collagen (2, 25) and in completely synthetic hyaluronic acid (HA)-based hydrogel (3) (Fig. 3A and SI Appendix, Fig. S10). We speculated that derived EVCs would be able to form vascular networks in a 3D matrix. Indeed, in both hydrogel systems, EVCs were found to form lavish networks (Fig. 3A); sorted VECad⁺ or VECad⁻ cells individually were unable to form such networks when encapsulated within collagen gels (Fig. 3B). VECad⁺ cells

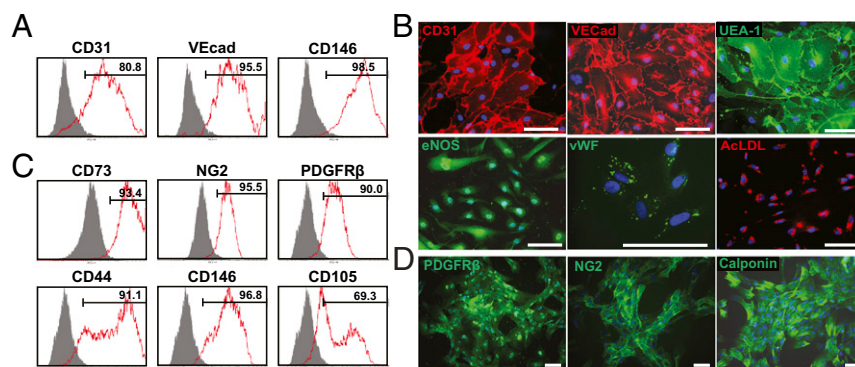


Fig. 2. EVC maturation. (A) Sorted VECad⁺ from hiPSC-BC1-derived EVCs subcultured for an additional 6 d in 50 ng/mL VEGF and SB431542-supplemented conditions and analyzed for the expression of VECad, CD31, and CD146 (representative flow cytometry plots; $n = 3$). (B) Subcultured sorted VECad⁺ from hiPSC-BC1-derived EVCs exhibited membrane localization of CD31 and VECad (both in red), lectin binding (in green), cytoplasmic expression of eNOS, punctuated vWF, and uptake of acLDL (in red). (C) hiPSC-BC1-derived EVCs subcultured for an additional 6 d in pericyte-inducing conditions (19) were analyzed for the expression of NG2, CD73, PDGFR β , CD44, CD146, and CD105 via flow cytometry. (D) Immunofluorescence analysis revealed appropriate localization of PDGFR β , NG2, and calponin (all in green). Isotype controls for flow cytometry are in gray, and nuclei are in blue. Results shown are typical of the independent experiments. (Scale bars: 100 μ m.)

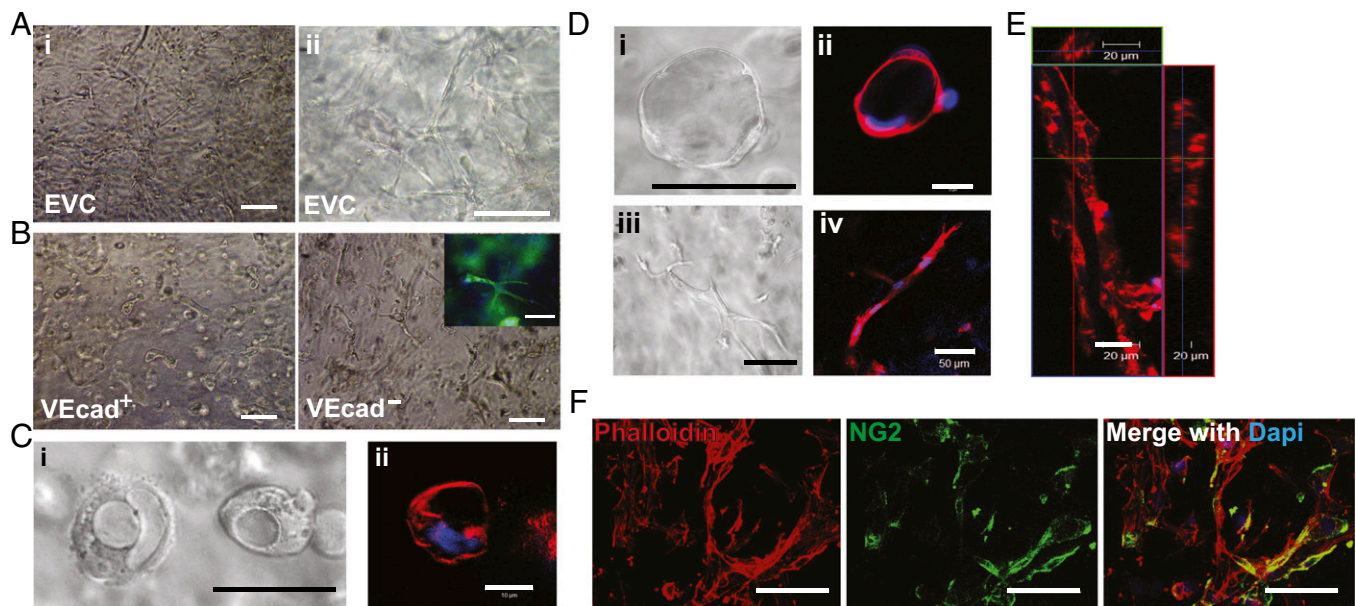


Fig. 3. Self-assembly of EVCs to multicellular networks in a 3D matrix. (A) Network formation from BC1-EVCs in collagen (i) and HA hydrogels (ii). (B) Sorted VEcad⁺ and VEcad⁻ cells encapsulated within collagen gels were unable to form networks. (Insert) Example of a cell with typical stellate morphology, with phalloidin in green and nuclei in blue. (Scale bars: 100 μm .) (C) Vacuole formation was observed after one day as evidenced by light microscopy (LM) (i) and confocal images (ii) of vacuole vital stain, FM4-64, in red and nuclei in blue. (Scale bar: 10 μm .) (D) On day 2, network formation with enlarged lumen (i and ii) and cell sprouting (iii and iv) were visualized by LM images (i and iii) and confocal images (ii and iv) of FM4-64 in red and nuclei in blue. (Scale bars: 10 μm in i and iii; 20 μm in ii; 50 μm in iv.) (E) On day 3, complex networks were observed with enlarged and open lumen, as indicated by confocal z-stacks and orthogonal sections of FM4-64 in red and nuclei in blue. (Scale bar: 20 μm .) (F) After 3 d, multilayered structures were also detected, as demonstrated by a 3D projection image of NG2 (green), phalloidin (red), and nuclei (blue) showing NG2⁺ pericytes integrated onto hollow structures. Images shown are typical of the independent experiment. (Scale bars: 50 μm .)

formed primarily vacuoles and started to form nascent structures within the collagen gel, with some instances of sprouting (Fig. 3B).

We attribute the lack of robust network formation from derived ECs in collagen gels to the lack of pericytes in culture, and speculate that the addition of support cells help form the networks seen with EVC encapsulation. VEcad⁻ cells exhibited cell spreading and a characteristic stellate morphology, but no network formation (Fig. 3B).

Vascular Morphogenesis of EVCs Within HA Hydrogels. We next examined the progress of EVC network formation within the HA hydrogel, a xeno-free synthetic construct engineered to recapitulate tubulogenesis-inducing signals (3). In vitro assessment of cellular behavior revealed the formation of multicellular networks via a sequential process typical of vascular morphogenesis. After 1 d of culture, we observed vacuole formation in many, but not all, of the cells. Some of these vacuoles had coalesced into a larger structure, resembling lumen (Fig. 3C and *SI Appendix*, Fig. S114).

To elucidate the phenotype of either cell type after 1 d, we also encapsulated VEcad⁺ and VEcad⁻ subpopulations independently. After 1 d, we clearly observed vacuoles in the encapsulated sorted VEcad⁺ subpopulation after 1 d; however, encapsulated sorted VEcad⁻ cells primarily spread, with no vacuole formation (*SI Appendix*, Fig. S11 B and C).

After 2 d of EVC encapsulation, we observed the progression of tubulogenesis, including extensive sprouting and an occasional open lumen (Fig. 3D and *SI Appendix*, Fig. S12A). By day 3, vascular networks had grown, with comprehensive multicellular networks clearly visible within HA hydrogels. Complex vascular networks with patent lumen structures were readily detected throughout the hydrogels, suggesting an engineered vascular network (Fig. 3E and *SI Appendix*, Fig. S12B). Interestingly, on

day 3, we detected NG2⁺ pericytes incorporated in the luminal structures and encircling the emerging tubular structures (Fig. 3F and *SI Appendix*, Fig. S13).

Integration of hPSC-Bicellular Microvascular Constructs. In vivo integration of vascular networks is crucial to the success of derived EVCs in regenerative medicine applications. We first tested whether EVCs can survive implantation, assemble into microvascular networks, integrate with the host vasculature, and establish blood flow. A Matrigel plug assay (5) revealed EVCs incorporated with perfused host microvasculature and generated human-only microvascular structures (*SI Appendix*, Fig. S14).

Next, to harness the self-organizing capability of EVCs in HA hydrogels, we implanted the engineered microvascular networks *s.c.* and assessed their survival and integration after 2 wk. We found that EVCs (derived from a BC1 or GFP-hiPSC cell line) were incorporated into or wrapped around the mouse microvasculature (Fig. 4 A and B and *SI Appendix*, Fig. S15), and that the hydrogels were largely degraded by 2 wk. HA gels without encapsulated cells exhibited slower remodeling and degradation *in vivo* compared to gels with cells, as we reported previously (3). Perfused microvasculature (as indicated by tail-injected, mouse-specific fluorescein-conjugated *GS-IB4* lectin) containing human ECs (with cross-sectional areas ranging from 100 to 25,000 μm^2) were abundant throughout the explant (~ 15 vessels per mm^2), demonstrating that the transplanted human vascular networks had anastomosed with the host circulatory systems (Fig. 4 C–E). Moreover, NG2⁺ human pericytes were found to migrate toward and encircle the perfused vasculature (Fig. 4F and *SI Appendix*, Fig. S16).

Although our bicellular constructs present several fundamental advancements to the future of cell-based therapies, additional studies are needed to fine-tune the ratio of early ECs to pericytes within EVC populations, owing to the wide variability of this

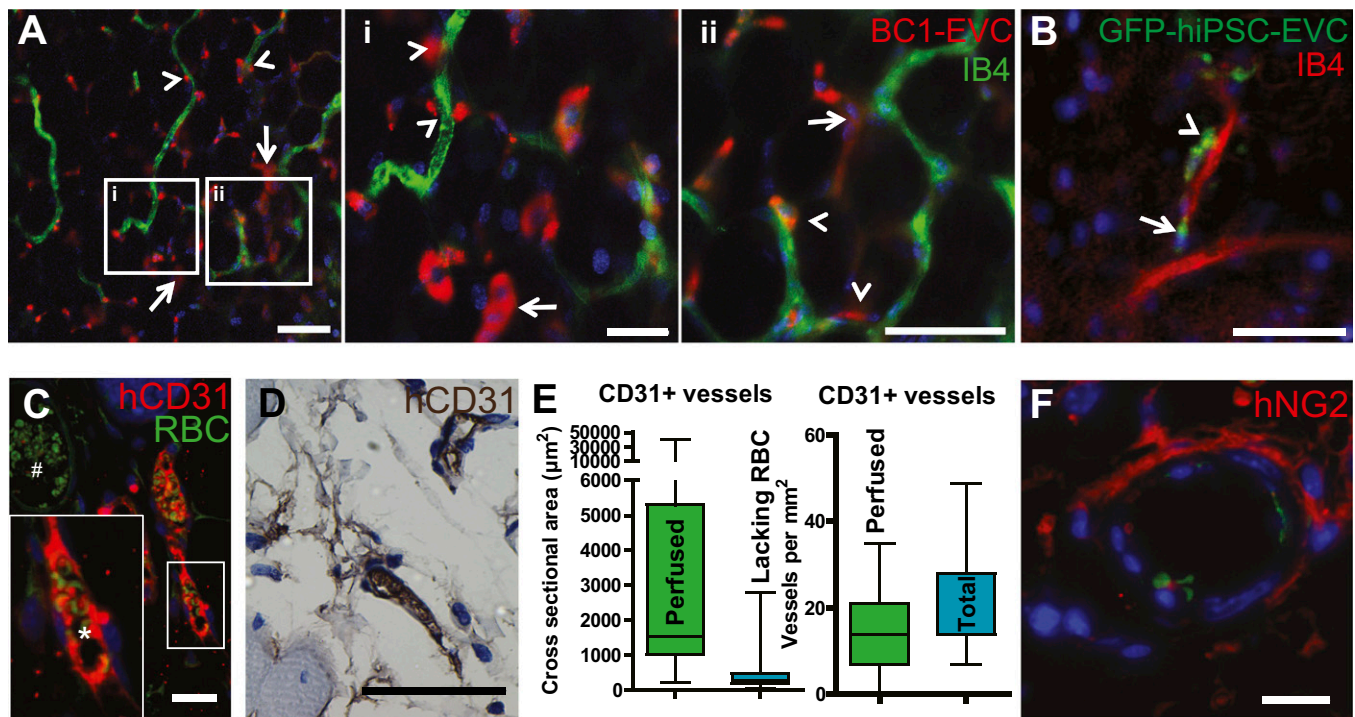


Fig. 4. Perfusion of EVC networks in vivo in synthetic hydrogels. (A and B) Confocal images of 2-wk explants of BC1-EVC (A) or GFP-hiPSC-EVC (B) networks in HA hydrogels demonstrate incorporation of human cells (A, red; B, green; arrows) into host vessels (tail vein-injected, mouse-specific Alexa Fluor 488-conjugated (A) or Alexa Fluor 546-conjugated (B) *GS-IB4* lectin and human cells exhibiting pericyte behavior (arrowheads). (Scale bars: 50 μm.) (i and ii) High-magnification views of indicated regions. (C and D) Histological examination of the explants stained for human specific CD31 expression via immunofluorescence (CD31 in red; RBCs in green; DAPI in blue) (C) and immunohistochemistry (CD31 in brown, counterstain in blue) reveals functional vessels containing human CD31⁺ cells with perfused blood cells (D). *Perfused human vessel; #perfused mouse vessel. (Scale bars: 10 μm in C; 50 μm in D.) (E) Quantification of cross-sectional areas and vessels per mm² of microvasculature containing human CD31⁺ cells depicts large perfused vessels and smaller vessels lacking RBCs in explants. (F) Immunofluorescence staining of sectioned explants for human specific NG2⁺ (red) cells reveals functional human pericytes wrapping perfused vessels. RBCs are in green, and DAPI is in blue. (Scale bar: 10 μm.)

ratio in different tissues and organs (26). Further investigation is also needed for clinical translation, including understanding of cell–cell interactions and appreciation of the longevity and durability of the human vascular networks. Future studies should focus on determining the in vivo longevity of engineered human networks to reveal not only the long-term integration of the human vasculature in the tissue, but also whether teratoma formation is of concern, a vital consideration of pluripotent stem cell therapies.

The balance between commitment and plasticity of the EVCs specifically within the vascular lineage allows for vascular fate and network maturation. This controlled system is reproducible, generates physiologically relevant vascular networks in implantable matrices, and thus provides the next fundamental step toward patient-specific engineered tissue with clinically translatable potential.

Experimental Procedures

Detailed descriptions of the materials and methods used in this study are provided in *SI Appendix, Materials and Methods*.

hPSC Culture. The hESC lines H9 and H13 (passages 15–40; WiCell Research Institute) and hiPSC lines MR31 (27), MMW2 (28), BC1 (29, 30), and a GFP transgenic hiPSC line (clone 26 hCBiPS aMHCneoPGKhygro + pCAGGS2 passage 47+10, kindly provided by Dr. Ulrich Martin, Hannover Medical School, Hannover, Germany) (31) were cultured as described previously (13, 32). Cell lines were routinely examined for pluripotent markers using immunofluorescence staining and flow cytometry analysis for TRA-1-60, TRA-1-81, stage-specific embryonic antigen-4 (SSEA4), and Oct4. Details of the various hPSCs are provided in *SI Appendix, Table S1*.

Differentiation Protocol. hPSCs were collected through digestion with EDTA (Promega), separated into an individual cell suspension using a 40-μm mesh strainer (BD Biosciences), and plated onto collagen IV (Trevigen)-coated plates at a concentration of 5×10^4 cells/cm². Cells were cultured for 6 d in a differentiation medium composed of alpha-MEM (Invitrogen), 10% FBS (HyClone), and 0.1 mM β-mercaptoethanol (β-ME), with the medium changed daily. On day 6, differentiated cells were collected through digestion with TrypLE (Invitrogen), separated with a 40-μm mesh strainer, and seeded at a concentration of 1.25×10^4 cells/cm² on collagen type IV-coated plates in endothelial cell growth media (ECGM) (PromoCell) supplemented with 2% FBS, 50 ng/mL VEGF with or without 10 μM SB431542 (Tocris), or 1 ng/mL VEGF plus 10 μM SB431542, for 6 d. The medium was changed every other day.

To elucidate whether serum-free conditions could be used to derive EVCs, we followed the aforementioned protocol, except differentiating the cells in alpha-MEM media supplemented with 20% knockout serum replacement, 0.1 mM β-ME, 1× nonessential amino acids (Gibco), and 1× L-glutamine (Invitrogen) for 6 d, followed by 6 d in ECGM base media (Promocell) supplemented with 50 ng/mL VEGF, 10 μM SB431542, 10% knockout serum replacement, β-ME, essential amino acids, and glutamine. These conditions were used only when specified in the text for serum-free differentiation.

EC Maturation. On day 12, derived EVCs were either subcultured in EC differentiation medium or sorted for VEcad⁺ cells. For the latter, EVCs were collected through digestion with magnetic activated cell sorting (MACS) buffer (0.5 M EDTA and 1% BSA in PBS), incubated with 10 μL of anti-human PE-conjugated VEcad (BD Biosciences) in MACS buffer for 45 min on ice, washed, incubated again with 20 μL of anti-PE microbeads (Miltenyi Biotec) in 80 μL of MACS buffer for 15 min at 4 °C, and finally washed twice. Cells were resuspended in 500 μL of MACS buffer and separated using a MS MACS separation column (Miltenyi Biotec). VEcad enrichment or depletion was confirmed by flow cytometry. Sorted cells were cultured on collagen type

IV-coated dishes for an additional 6 d in ECGM supplemented with 50 ng/mL VEGF and 10 μ M SB431542. The medium was changed every other day.

Pericyte Maturation. We followed a published protocol for pericyte maturation (19). On day 12, derived EVCs were collected through digestion with TrypLE and replated on tissue culture-treated six-well plates in medium composed of DMEM and 10% FBS. After 2–3 h, unattached cells were removed, and the medium was replaced. Cells were cultured for 6 d, with the medium changed every other day.

HA Gels. Acrylated HA hydrogels were prepared as reported previously (3, 33, 34). Derived EVCs or sorted subpopulations were encapsulated in HA hydrogels at a density of 4×10^6 cells/mL and cultured for up to 3 d in endothelial growth media 2 (EGM2; Lonza). Visualization and image acquisition were performed using an inverted light microscope (Olympus) and a confocal microscope (Zeiss LSM 510 Meta) along the culture. FM-464 vacuole staining (Invitrogen) was performed following the manufacturer's protocol (3). To test parallel differentiation, EVCs were also cultured in adherent culture in EGM2 for 3 d, with daily medium changes.

Implantation of Cells. Except for GFP-hiPSC-derived cells, all other PSCs (hiPSC-MR31, hESC-H9, hiPSC-BC1)-derived cells were labeled with PKH-26 (red) according to the manufacturer's protocol and as described previously (13). PKH-26-labeled cells were resuspended with Matrigel and 50 ng/mL bFGF or engineered vascular networks in HA gels for 3 d, then implanted s.c. into nude 6- to 8-wk-old female mice in quadruplicate. To visualize

angiogenesis in the implants before sample removal after 2 wk, we injected Alexa Fluor 488 (or in some cases, Alexa Fluor 546 or 647)-conjugated isolectin GS-IB4 from *Griffonia simplicifolia* (Invitrogen) through the tail veins of the mice (35). After 20 min, mice were euthanized by CO₂ asphyxiation, after which the explants were harvested and fixed in 3.7% formaldehyde (Sigma-Aldrich) and proceeded for visualization and sectioning. The Johns Hopkins University's Institutional Animal Care and Use Committee approved all animal protocols.

Graphs and Statistics. All analyses were performed in triplicate samples for $n = 3$ at least. Quantitative RT-PCR was also performed on triplicate samples ($n = 3$) with triplicate readings. One-way ANOVA with the Bonferroni post hoc test were performed to determine significance using GraphPad Prism 4.02.

ACKNOWLEDGMENTS. We thank M. Wanjare for input on smooth muscle lineage differentiation; S. H. Tan, E. Peijnenburg, P. Patel, B. Macklin, and S. Zhao for technical assistance; S. Khetan and J. Burdick (University of Pennsylvania) for HA; Z. Binder for assistance with immunohistochemistry; Y. J. Kim and G. Lee for input on neuronal markers and providing the positive control; K. Schwanke and M. Ulrich (Hannover Medical School) for kindly providing GFP transgenic hiPSCs; and D. Hutton and W. L. Grayson for their expertise and assistance with adipogenic and osteogenic differentiations. This work was supported by predoctoral awards from the American Heart Association and National Institutes of Health (NIH) Grant F31HL112644 (both to S.K.), NIH Grant 2R01 HL073781 (to L.C.), NIH Grants R01 HL107938 and U54CA143868, an American Heart Association Scientist Development grant, and National Science Foundation Grant 1054415 (to S.G.).

- Discher DE, Mooney DJ, Zandstra PW (2009) Growth factors, matrices, and forces combine and control stem cells. *Science* 324(5935):1673–1677.
- Stratman AN, Malotte KM, Mahan RD, Davis MJ, Davis GE (2009) Pericyte recruitment during vasculogenic tube assembly stimulates endothelial basement membrane matrix formation. *Blood* 114(24):5091–5101.
- Hanjaya-putra D, et al. (2011) Controlled activation of morphogenesis to generate a functional human microvasculature in a synthetic matrix. *Blood* 118(3):804–815.
- Vunjak-Novakovic G, Scadden DT (2011) Biomimetic platforms for human stem cell research. *Cell Stem Cell* 8(3):252–261.
- Ferreira LS, et al. (2007) Vascular progenitor cells isolated from human embryonic stem cells give rise to endothelial and smooth muscle-like cells and form vascular networks in vivo. *Circ Res* 101(3):286–294.
- Park S-W, et al. (2010) Efficient differentiation of human pluripotent stem cells into functional CD34⁺ progenitor cells by combined modulation of the MEK/ERK and BMP4 signaling pathways. *Blood* 116(25):5762–5772.
- Yang L, et al. (2008) Human cardiovascular progenitor cells develop from a KDR⁺ embryonic stem cell-derived population. *Nature* 453(7194):524–528.
- Vodyanik MA, et al. (2010) A mesoderm-derived precursor for mesenchymal stem and endothelial cells. *Cell Stem Cell* 7(6):718–729.
- Wang ZZ, et al. (2007) Endothelial cells derived from human embryonic stem cells form durable blood vessels in vivo. *Nat Biotechnol* 25(3):317–318.
- James D, et al. (2010) Expansion and maintenance of human embryonic stem cell-derived endothelial cells by TGF β inhibition is Id1 dependent. *Nat Biotechnol* 28(2):161–166.
- Drukker M, et al. (2012) Isolation of primitive endoderm, mesoderm, vascular endothelial and trophoblast progenitors from human pluripotent stem cells. *Nat Biotechnol* 30(6):531–542.
- Rufaihah AJ, et al. (2013) Human induced pluripotent stem cell-derived endothelial cells exhibit functional heterogeneity. *Am J Transl Res* 5(1):21–35.
- Wanjare M, Kuo F, Gerecht S (2013) Derivation and maturation of synthetic and contractile vascular smooth muscle cells from human pluripotent stem cells. *Cardiovasc Res* 97(2):321–330.
- Dar A, et al. (2012) Multipotent vasculogenic pericytes from human pluripotent stem cells promote recovery of murine ischemic limb. *Circulation* 125(1):87–99.
- Duff SE, Li C, Garland JM, Kumar S (2003) CD105 is important for angiogenesis: Evidence and potential applications. *FASEB J* 17(9):984–992.
- Bardin N, et al. (2001) Identification of CD146 as a component of the endothelial junction involved in the control of cell-cell cohesion. *Blood* 98(13):3677–3684.
- Airas L, et al. (1995) CD73 is involved in lymphocyte binding to the endothelium: Characterization of lymphocyte-vascular adhesion protein 2 identifies it as CD73. *J Exp Med* 182(5):1603–1608.
- Crisan M, et al. (2008) A perivascular origin for mesenchymal stem cells in multiple human organs. *Cell Stem Cell* 3(3):301–313.
- Orlidge A, D'Amore PA (1987) Inhibition of capillary endothelial cell growth by pericytes and smooth muscle cells. *J Cell Biol* 105(3):1455–1462.
- Gerecht-Nir S, Ziskind A, Cohen S, Itskovitz-Eldor J (2003) Human embryonic stem cells as an in vitro model for human vascular development and the induction of vascular differentiation. *Lab Invest* 83(12):1811–1820.
- Yamashita J, et al. (2000) Flk1-positive cells derived from embryonic stem cells serve as vascular progenitors. *Nature* 408(6808):92–96.
- White MP, et al. (2013) Limited gene expression variation in human embryonic stem cell and induced pluripotent stem cell-derived endothelial cells. *Stem Cells* 31(1):92–103.
- Wang L, et al. (2004) Endothelial and hematopoietic cell fate of human embryonic stem cells originates from primitive endothelium with hemangioblastic properties. *Immunity* 21(1):31–41.
- Crisan M, Corselli M, Chen WC, Péault B (2012) Perivascular cells for regenerative medicine. *J Cell Mol Med* 16(12):2851–2860.
- Stratman AN, et al. (2009) Endothelial cell lumen and vascular guidance tunnel formation requires MT1-MMP-dependent proteolysis in 3-dimensional collagen matrices. *Blood* 114(2):237–247.
- Armulik A, Abramsson A, Betsholtz C (2005) Endothelial/pericyte interactions. *Circ Res* 97(6):512–523.
- Mali P, et al. (2010) Butyrate greatly enhances derivation of human induced pluripotent stem cells by promoting epigenetic remodeling and the expression of pluripotency-associated genes. *Stem Cells* 28(4):713–720.
- Zou J, Mali P, Huang X, Dowey SN, Cheng L (2011) Site-specific gene correction of a point mutation in human iPSC cells derived from an adult patient with sickle cell disease. *Blood* 118(17):4599–4608.
- Chou BK, et al. (2011) Efficient human iPSC cell derivation by a non-integrating plasmid from blood cells with unique epigenetic and gene expression signatures. *Cell Res* 21(3):518–529.
- Cheng L, et al.; NISC Comparative Sequencing Program (2012) Low incidence of DNA sequence variation in human induced pluripotent stem cells generated by non-integrating plasmid expression. *Cell Stem Cell* 10(3):337–344.
- Haase A, et al. (2009) Generation of induced pluripotent stem cells from human cord blood. *Cell Stem Cell* 5(4):434–441.
- Vo E, Hanjaya-putra D, Zha Y, Kusuma S, Gerecht S (2010) Smooth-muscle-like cells derived from human embryonic stem cells support and augment cord-like structures in vitro. *Stem Cell Rev* 6(2):237–247.
- Khetan S, Burdick JA (2010) Patterning network structure to spatially control cellular remodeling and stem cell fate within 3-dimensional hydrogels. *Biomaterials* 31(32):8228–8234.
- Khetan S, Katz JS, Burdick JA (2009) Sequential crosslinking to control cellular spreading in 3-dimensional hydrogels. *Soft Matter* 5(8):1601–1606.
- Kang K-T, Allen P, Bischoff J (2011) Bioengineered human vascular networks transplanted into secondary mice reconnect with the host vasculature and re-establish perfusion. *Blood* 118(25):6718–6721.
- Lee G, Chambers SM, Tomishima MJ, Studer L (2010) Derivation of neural crest cells from human pluripotent stem cells. *Nat Protoc* 5(4):688–701.

SI APPENDIX

SI Materials and Methods

hPSC culture. Human ESC line H9 (passages 15 to 40; WiCell Research Institute, Madison, WI) and hiPSC lines MR31 (1), BC1 (2-3), and a GFP transgenic hiPSC line (Clone 26 hCBiPS aMHCneoPGKhygro + pCAGGS2 Passage 47+10, kindly provided by Dr. Ulrich Martin, Hannover Medical School, Germany) (4) were cultured as previously described (5-6). Cell lines were routinely examined for pluripotent markers using immunofluorescence staining and flow cytometry analysis for TRA-1-60, TRA-1-81, SSEA4, and Oct4. See **Table S1** for details on the various hPSCs.

Differentiation protocol. Human PSCs were collected through digestion with ethylenediaminetetraacetic acid (EDTA; Promega), separated into an individual cell suspension using a 40- μ m mesh strainer (BD Biosciences), and plated onto collagen IV (Trevigen) coated plates at a concentration of 5×10^4 cells/cm². Cells were cultured for 6 days in a differentiation medium composed of alpha-MEM (Invitrogen), 10% FBS (Hyclone) and 0.1 mM β -mercaptoethanol (β -ME), with the media changed daily. On day 6, differentiated cells were collected through digestion with TrypLE (Invitrogen), separated with a 40- μ m mesh strainer, and seeded at a concentration of 1.25×10^4 cells/cm² on collagen-type-IV-coated plates in endothelial cell growth media (ECGM) (PromoCell) supplemented with 2% FBS, 50ng/ml VEGF with or without 10 μ M SB431542 (Tocris), or 1ng/ml VEGF + 10 μ M SB431542, as described in the text for 6 days. Media was changed every other day. To elucidate whether serum-free conditions could be used to derive EVCs, we followed the aforementioned protocol except differentiating the cells in alpha-MEM media supplemented with 20% knockout serum replacement, 0.1 mM β -ME, 1x non-essential amino acids (Gibco), and 1X L-glutamine (Invitrogen) for 6 days, followed by 6 days in ECGM base media (Promocell) supplemented with 50ng/ml VEGF, 10 μ M SB431542, 10% knockout serum replacement, β -ME, essential amino acids, and glutamine. These conditions were used only where specified in the text.

Flow cytometry. Flow cytometry was performed as previously described (7). Briefly, cells were incubated with FITC- or PE-conjugated antigen specific antibodies for markers outlined in the text (**Table S2**). All analyses were done using corresponding isotype controls. Forward-side scatter plots were used to exclude dead cells. User guide instructions were followed to complete the flow cytometry analysis via Cyflogic v1.2.

Real-time quantitative RT-PCR. Two-step reverse transcription polymerase chain reaction (RT-PCR) was performed on differentiated and undifferentiated (day 0) hPSCs as previously described in accordance with Applied Biosystems manufacturer instructions (7). For each primer set (*VEcad*, *SMMHC*, *Tuj1*, *peripherin*, and *ICAM*), we used the comparative computerized tomography method (Applied Biosystems) to calculate the amplification differences between different samples. The values for experiments were averaged and graphed with standard deviations.

Immunofluorescence. Cells were prepared for immunofluorescence as previously described (7). Briefly, fixed cells were blocked in 1% BSA, treated with 0.1% Triton-X (Sigma), and incubated with the antigen specific antibodies for the markers outlined in the text (**Table S2**), followed by

an appropriate secondary, and DAPI (Roche Diagnostics). The immunolabeled cells were examined using a fluorescent microscope (Olympus BX60).

EC maturation. On day 12, derived EVCs were either sub-cultured in differentiation medium or sorted for VEcad⁺ cells. For this, EVCs were collected through digestion with Magnetic Activated Cell Sorting (MACS) buffer (0.5M EDTA and 1% BSA in PBS), incubated with 10ul anti-human, PE-conjugated VEcad (BD) in MACS buffer for 45 minutes on ice, washed, incubated with 20 ul anti-PE microbeads (Miltenyi Biotec) in 80ul MACS buffer for 15 minutes at 4°C, and washed twice. Cells were re-suspended in 500µl MACS buffer and separated using a MS MACS separation column (Miltenyi Biotec). VEcad enrichment or depletion was confirmed by flow cytometry. Sorted cells were cultured on collagen-type-IV-coated dishes for an additional 6 days in ECGM supplemented with 50ng/ml VEGF and 10µM SB431542. Media was changed every other day.

Dil-labeled Ac-LDL uptake. Derived ECs were incubated with 10 µg/ml Dil-labeled Ac-LDL (Invitrogen) for 4 hours at 37°C, rinsed three times with PBS, fixed with 4% paraformaldehyde for 30 minutes, and visualized using a fluorescence microscope (Olympus).

Tumor Necrosis Factor alpha (TNF-α) activation. A previously established protocol for the activation of ECs was used (8). Briefly, cultured cells were stimulated for 24 hours with 10 ng/ml tumor necrosis factor-alpha (TNF-α; R&D) or blank as a control and analyzed for *ICAM* (Applied Biosystems).

Matrigel cord formation. Cells were labeled with PKH-26 (red) according to the manufacturer's protocol. Briefly, cells were mixed with diluents C and PKH-26 for 5 minutes. The reaction was stopped by adding Hyclone FBS and the cells were washed three times. Cells were observed for their ability to form cord structures on Matrigel (BD Bioscience) as previously described (5). Briefly, Matrigel was cast into µ-Slide Angiogenesis wells (iBidi, Munich, Germany). After polymerization, 20,000 PKH-stained cells were seeded per well. Visualization and image acquisition were performed using fluorescence microscopy (Olympus BX60) after 24 hours.

Pericyte maturation. We followed a published protocol for pericyte maturation (9). Briefly, On day 12, derived EVCs were collected through digestion with TrypLE and re-plated on tissue culture treated 6 well plates in media comprised of DMEM and 10% FBS. After 2-3 hours, unattached cells were removed and media was replaced. Cells were cultured for 6 days, changing the media every second day.

Mesenchymal differentiation (adipogenic and osteogenic). For adipogenic differentiation (10), we cultured derived pericytes at 10,000cells/cm² in media comprised of DMEM, 10% FBS, 1% Penicillin/Streptomycin, 200µM Indomethacin, 500 µM 3-Isobutyl-1-methyl xanthine (IBMX), and 5 µg/ml Insulin (all from Sigma) for 4 weeks. To assess adipogenic potential, cells were fixed with 3.7% formaldehyde, then dehydrated with 60% isopropanol for 5 minutes. Cells were incubated with Oil Red O (Sigma) at 1.8 mg/ml in 60/40 isopropanol/DI H₂O, for 10 minutes and imaged using an inverted light microscope (Olympus).

For osteogenic differentiation (11), we cultured derived pericytes at 5,000cells/cm² in media comprised of low glucose DMEM, 10% FBS, 1% Penicillin/Streptomycin, 10mM β-

glycerophosphate, 100nM dexamethasone, and 50 μ M ascorbic acid (all from Sigma) for 2 weeks. Media were prepared fresh weekly. To assess osteogenic potential, samples were fixed with 3.7% formaldehyde, and washed with DI H₂O. Samples were incubated with Alizarin Red S (40mM in DI H₂O, pH ~4.2; Sigma) for 10-20 minutes.

Collagen gel assay. Stock solution was used to prepare collagen gels at a density of 2.5 mg/ml, as previously described in the literature. Gel formation was achieved by simultaneously decreasing the solution's pH and increasing the temperature to 37°C. To prepare 1 ml of 2.5 mg/ml collagen gel, we added 2 million derived cells (EVCs, VEcad⁺ cells, or VEcad⁻ cells) resuspended in 200 μ l M199 [1X] to a mixture of 39 μ l M199 [10x] + 400.6 μ l M199 [1X]. To this, we added 350 μ l Collagen Type I. After the addition of approximately 10 μ l of 1M NaOH, the solution was thoroughly mixed and transferred to wells of a 96 well plate. ECGM supplemented with 50ng/ml VEGF was added to the gels after 30 minutes at 37°C in a CO₂ incubator. Visualization and image acquisition were performed using an inverted light microscope (Olympus).

Synthesis of HA gels. Acrylated HA (AHA) hydrogels were prepared as previously reported (12-13). Briefly, AHA was synthesized using a two-step protocol: (1) the tetrabutylammonium salt of HA (HA-TBA) was formed by reacting sodium hyaluronate (64 kDa; Lifecore Biomedical, Chaska, MN) with the highly acidic ion exchange resin Dowex-100 and neutralizing with 0.2 M TBA-OH; (2) acrylic acid (2.5 Eq) was coupled to HA-TBA (1 Eq, repeat unit) in the presence of dimethylaminopyridine (DMAP; 0.075 Eq) and di-tert-butyl dicarbonate (1.5 Eq) in DMSO, followed by dialysis and lyophilization. ¹H NMR was used to confirm the final percent modification of the AHA.

Peptides. The cell adhesive peptide GCGYGRGDSPG (MW: 1025.1 Da; bold italics indicates the RGD integrin-binding domain) and matrix metalloproteinases (MMP) sensitive crosslinker GCRDGPQG↓IWGQDRCG (MW: 1754.0 Da; down arrow indicates the site of proteolytic cleavage) were obtained from GenScript Corporation (Piscataway), all with more than 95 percent purity (per manufacturer high-performance liquid chromatography analysis).

EVC, sorted VE-Cad⁺ and sorted VE-Cad⁻ subpopulation encapsulation and culture. AHA polymer (3 wt%) was dissolved in a sodium phosphate buffered saline (NaPBS buffer: 0.1 M sodium phosphate, 0.3 M total osmolarity, pH 8.0). The cell adhesive peptides (RGDS; GenScript) were dissolved in NaPBS buffer and added to the AHA solution at final peptide concentration of 3.7 mM and allowed to react for one hour with gentle shaking. Recombinant human VEGF₁₆₅ (Pierce), bFGF (Invitrogen), Ang-1 (R&D), tumor necrosis factor-alpha (TNF- α ; R&D) and stromal cell-derived factor-1 (SDF-1; R&D) were added at 50 ng/ml into the AHA-RGDS mixture. Derived EVCs or sorted subpopulations were encapsulated in HA hydrogels at a density of 4 X 10⁶ cells/ml. Following the resuspension of cells, the MMP solution was added at 4.83 mM (corresponding to the 25 percent of available acrylate groups within the 3 wt% AHA). Immediately after adding the MMP crosslinker, 40 μ l of this mixture was pipetted into sterile molds (5 mm diameter, 2 mm height) and allowed to react for 15 minutes at room temperature inside the laminar flow hood. The formed constructs were cultured for up to three days in endothelial growth media 2 (EGM2; Lonza). Visualization and image acquisition were performed using an inverted light microscope (Olympus) and a confocal microscope (LSM 510 Meta; Carl Zeiss) at various times during culture. We performed FM-464 vacuole staining

(Invitrogen) following the manufacturer's protocol. To test parallel differentiation, day 12 EVCs were also cultured in adherent culture in EGM 2 (Lonza) for 3 days with media changed daily.

Subcutaneous implantation of cells. Except for GFP-hiPSC derived cells, all other PSC-derived cells were labeled with PKH-26 (red) according to the manufacturer's instructions. Labeled cells, which were re-suspended with growth factor-reduced Matrigel (BD) and 50ng/ml bFGF or engineered vascular networks in HA gels for 3 days were implanted subcutaneously into nude 6-8 week old female mice in quadruplicate. To visualize angiogenesis in the implants prior to sample removal after 2 weeks, we injected Alexa Fluor(R) 488 (or, in some instances, AlexaFluor(R) 647 or 546) conjugated isolectin GS-IB4 from *Griffonia simplicifolia* (Invitrogen) through the tail veins of the mice (14). After 20 minutes, mice were euthanized by CO₂ asphyxiation and the explants were harvested and fixed in 3.7 percent formaldehyde (Sigma) and proceeded for visualization and sectioning. The Johns Hopkins University Institutional Animal Care and Use Committee approved all animal protocols.

Histology. The fixed explants were dehydrated in graded ethanol (70%-100%), embedded in paraffin, serially sectioned using a microtome (5 μ m), and stained with immunohistochemistry for anti-human CD31 (Dako) and anti-human NG2 (Santa Cruz) (15-16). Mouse tissue was used as controls. Blood vessels containing human CD31 cells were counted and measured for area using ImageJ (NIH). We sampled a minimum of 6 images for each construct.

Graphs and Statistics. All analyses were performed in triplicate samples for n=3 at least. Real-time RT-PCR were also performed on triplicate samples (n=3) with triplicate readings. One Way ANOVA with Bonferroni post-hoc test were performed to determine significance (GraphPad Prism 4.02).

Supplementary Figures

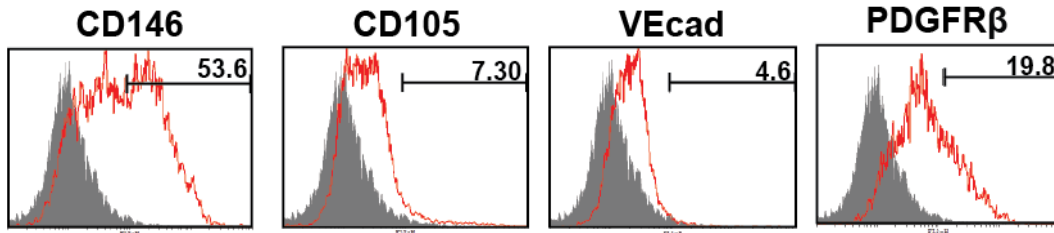


Fig. S1. Differentiating hPSCs. hiPSC-BC1 were differentiated in monolayer for 6 days and analyzed using flow cytometry analysis (n=3) for markers of interest including CD146, CD105, VEcad, and PDGFR β . Isotype controls for flow cytometry are in gray. Results shown are for hiPSC-BC1 cell line and typical of the independent experiments.

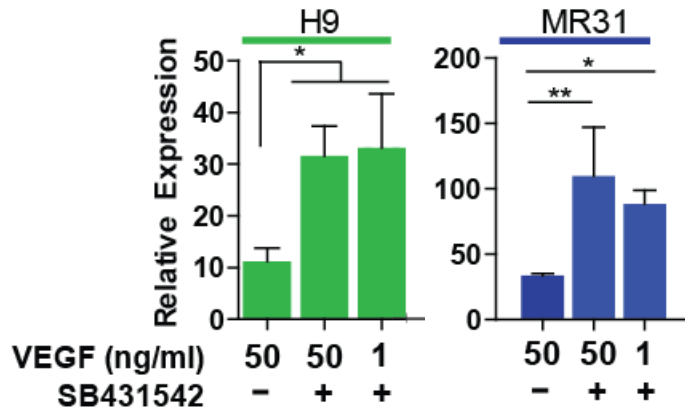


Fig. S2. The effect of VEGF and TGF β inhibitor on VEcad expression. hPSCs were differentiated in monolayer for 6 days followed by an additional 6 days in medium supplemented with and without SB431542 in low and high VEGF concentrations and analyzed using real-time PCR for VEcad expression (n=3). VEcad expression was upregulated with the addition of TGF β inhibitor independently of VEGF concentrations in all hPSC lines tested. Significance levels were set at *p<0.05, **p<0.01, and ***p<0.001. Data are reported \pm SEM.

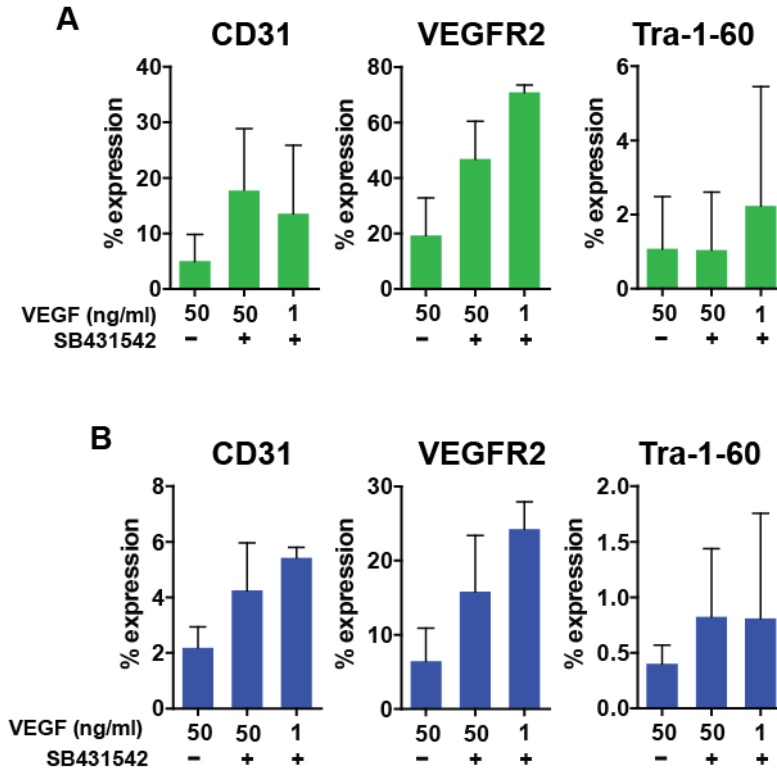


Fig. S3. The effect of VEGF and TGF β inhibitor on CD31, VEGFR2, and Tra-1-60 expression. hPSCs were differentiated in monolayer for 6 days followed by an additional 6 days in medium supplemented with and without SB431542 in low and high VEGF concentrations and analyzed using flow cytometry (n=3) for CD31, VEGFR2, and Tra-1-60 expression in **(A)** hESC-H9 and **(B)** hiPSC-MR31 lines. CD31 expression did not change in the different treatments, while VEGFR2 expression was upregulated in media supplemented with low VEGF concentration. Tra-1-60 expression was downregulated to <1% in conditions supplemented with high VEGF. Data are reported \pm SEM.

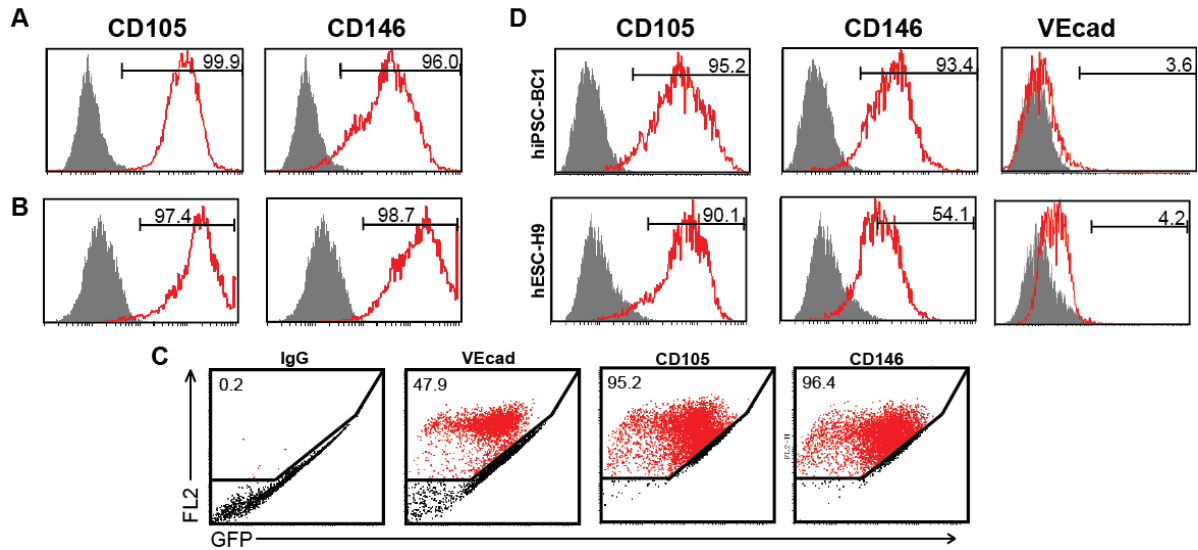


Fig. S4. Marker expression in EVCs. hPSCs were differentiated in monolayer for 12 days and EVC derivatives were analyzed using flow cytometry (n=3) assessing expression of CD105 and CD146 from (A) hiPSC-MR31 and (B) hESC-H9 differentiated cells. (C) EVCs were also derived from a GFP transgenic hiPSC line (4) and confirmed for their marker expression profile by flow cytometry. (D) Flow cytometry analysis of CD105, CD146, and VEcad in hPSCs differentiated for 12 days lacking supplementation of VEGF or SB431542. Isotype controls for flow cytometry are in gray. Results shown are typical of the independent experiments.

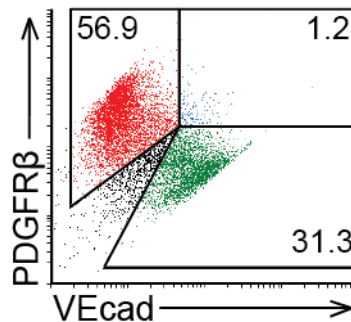


Fig. S5. PDGFR β and VEcad expression in H9 EVCs. H9-EVCs differentiated in media supplemented with SB431542 and using high VEGF concentrations were double labeled for PDGFR β and VEcad and analyzed via flow cytometry. Results shown are typical of the independent experiments.

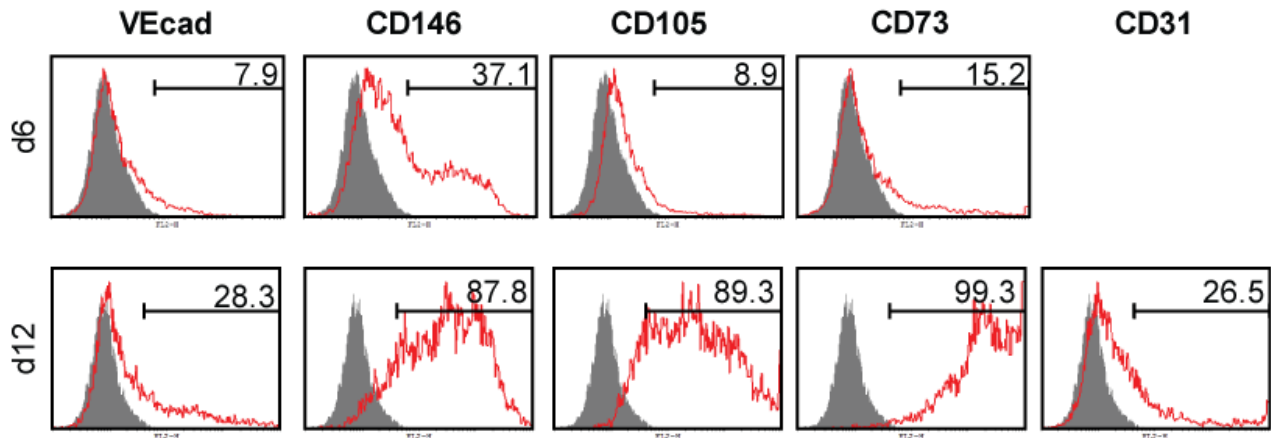


Fig. S6. EVCs derived using serum-free conditions. Flow cytometry (n=3) analysis of hiPSC-BC1-derivatives after 6 and 12 days of differentiation in serum-free conditions reveals marker expressions comparable to that of the standard differentiation scheme. Isotype controls for flow cytometry are in gray. Results shown are typical of the independent experiments.

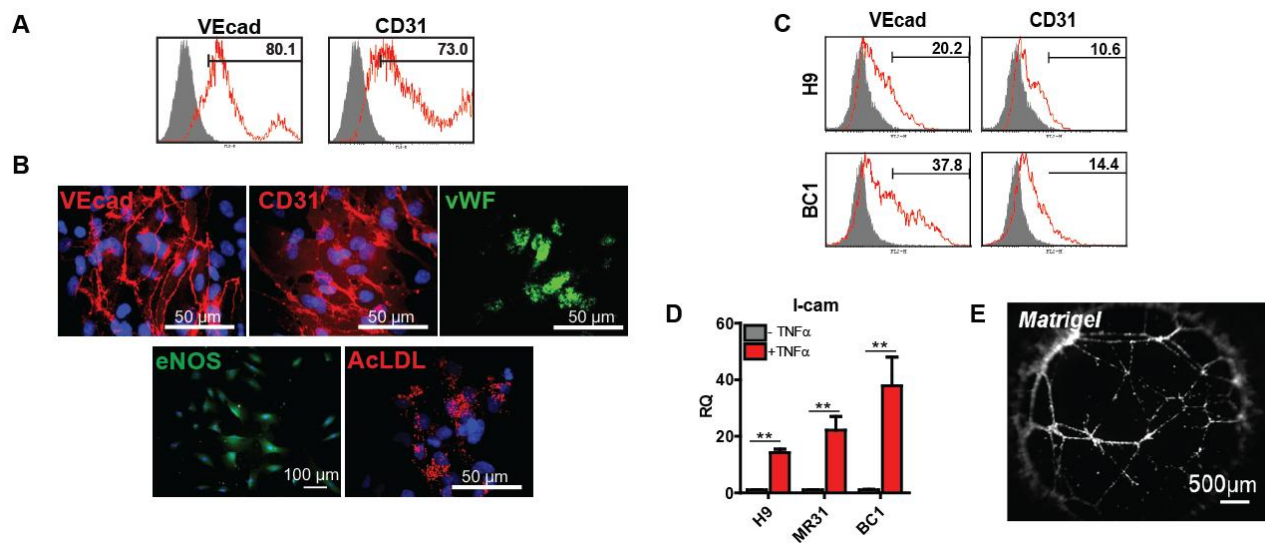


Fig. S7. EC maturation. hiPSC-MR31-derived EVCs were sub-cultured for an additional 6 days in 50ng/ml VEGF and SB431542-supplemented conditions and analyzed for (A) the expression of VECad and CD31 expression (representative flow cytometry plots; n=3); and (B) membrane localization of VECad and CD31 (both in red), cytoplasmic expression of vWF and eNOS (both in green) and uptake of acLDL (in red). Nuclei counterstained in blue. (C) Representative flow cytometry plots (n=3) of VECad and CD31 expression in hiPSC-BC1- and hESC-H9- derived EVCs subcultured for an additional 6 days in SB431542-supplemented conditions. Isotype controls for flow cytometry are in gray. (D-E) VECad⁺ cells from EVCs of the different hPSC-lines were sub-cultured for an additional 6 days in SB431542-supplemented conditions and analyzed for (D) the expression of I-cam in response to TNF α and (E) network formation on Matrigel (hiPSC-MR31). Significance levels were set at *p<0.05, **p<0.01, and ***p<0.001. Data are reported \pm SEM.

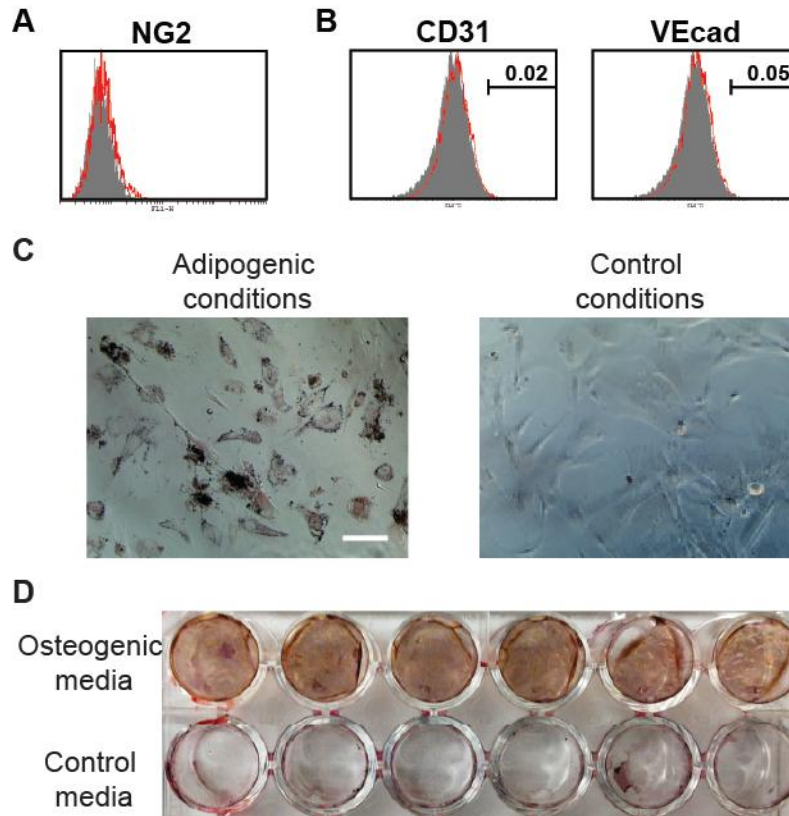


Fig. S8. Pericyte maturation and mesenchymal differentiation potential. (A) hiPSC-BC1-derived EVCs were negative for pericyte marker, NG2 (representative flow cytometry plots; n=3). (B) hiPSC-BC1-derived EVCs sub-cultured for an additional 6 days in pericyte-inducing conditions (9) were analyzed for the expression of CD31 and VEcad via flow cytometry (representative flow cytometry plots; n=3). Isotype controls for flow cytometry are in gray. Results shown are typical of the independent experiments. (C,D) Derived pericytes differentiated into mesenchymal lineages including (C) adipocytes (Oil Red O stain) and (D) osteoblasts (Alizarin Red S stain). Scale bar is 50 μ m.

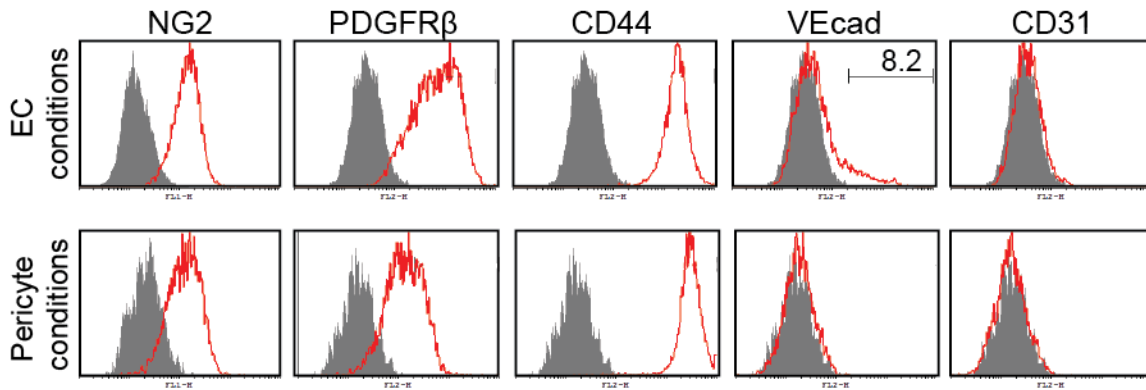


Fig. S9. Sorted VECad⁻ cells. Sorted VECad⁻ cells from hiPSC-BC1-derived EVCs sub-cultured for an additional 6 days in EC conditions (50ng/ml VEGF and SB431542) or pericyte maturation conditions analyzed for the expression of NG2, PDGFR β , CD44, VECad, and CD31 (representative flow cytometry plots; n=3). Isotype controls for flow cytometry are in gray. Results shown are typical of the independent experiments.

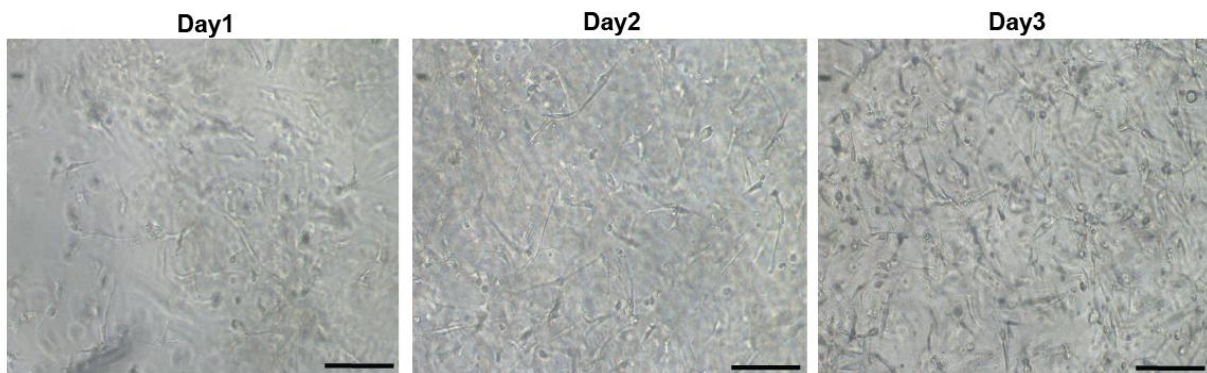


Fig. S10. Cord formation of EVCs in collagen gels. EVC derivatives (hESC-H9) were encapsulated in collagen gels and cord-like structure formation was observed along the culture period. Scale bars are 100 μ m.

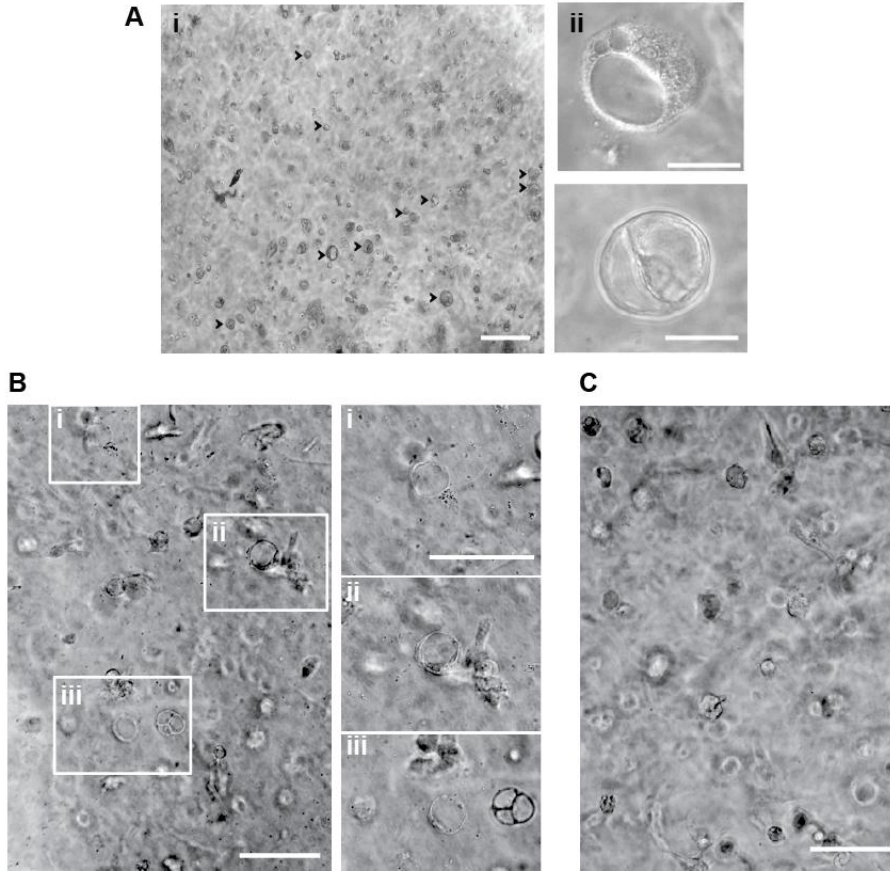


Fig. S11. Vacuole formation after 1 day HA encapsulation. BC1-EVCs were encapsulated in HA hydrogels and visualized via light microscopy after 1 day. (A) Vacuole formation on day 1 via (i) low magnification (scale bar=100μm; some vacuole are indicated by arrowheads) and (ii) high magnification of individual cells (scale bar is 5μm). (B) BC1-EVC sorted VEcad⁺ subpopulation encapsulated in HA gels were able to form vacuoles whereas (C) BC1- EVC sorted VEcad⁻ subpopulation were not. Scale bar in B, C are 10μm. Images shown are typical of the independent experiments.

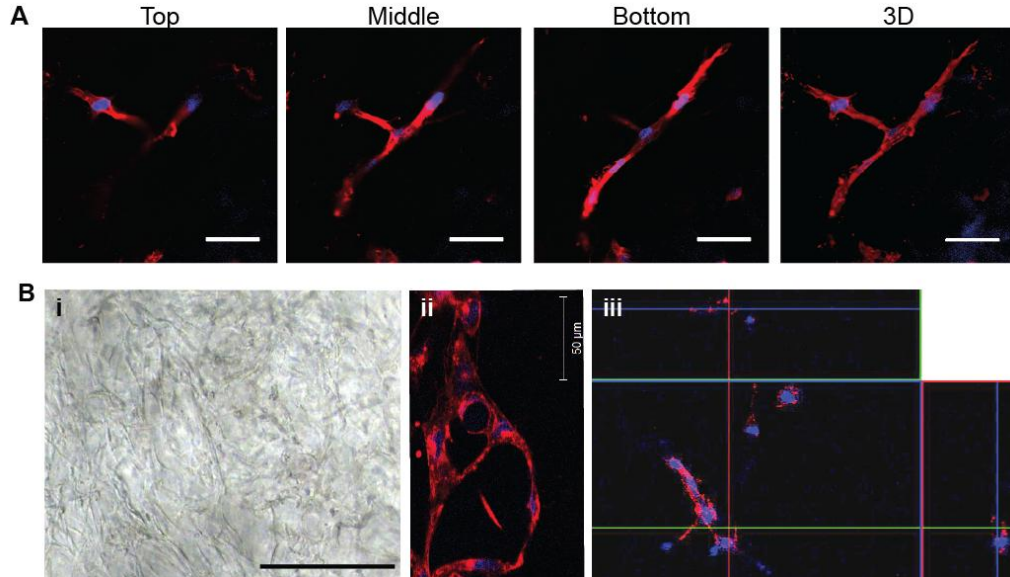


Fig. S12. Network formation of EVCs in HA matrix from day 2 to 3. BC1-EVCs were encapsulated in HA hydrogels and the kinetics of network formation was documented with (A) sprouting and initial network formation on day 2 as indicated by serial confocal z-stack images of vacuole vital stain, FM4-64 (red) and nuclei (blue) (scale bar is 50µm); and (B) complex networks on day 3 as indicated by (i) light microscopy (scale bar is 100µm), with enlarged and open lumen as indicated by (ii) confocal z-stacks and (iii) orthogonal sections of vacuole vital stain, FM4-64 (red) and nuclei (blue). Images shown are typical of the independent experiments.

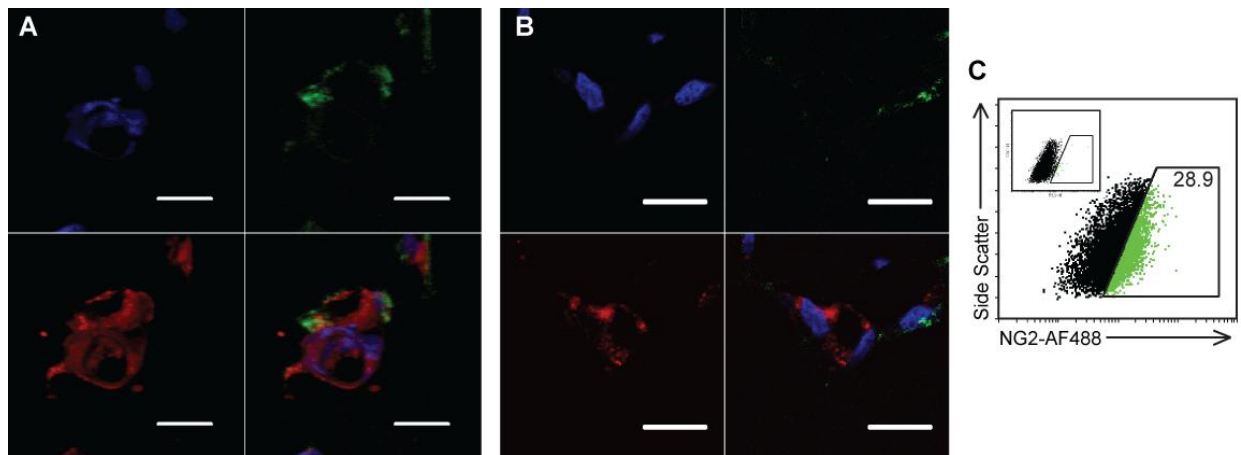


Fig. S13. Derived pericytes in the vascular networks. EVCs were encapsulated in HA hydrogels and after 3 days in culture, multilayer structures were detected as demonstrated by confocal microscopy of NG2 (green), vacuole vital stain FM4-64 (red), and nuclei (blue) showing (A) pericytes integrated onto a hollow tubular structure (3D projection) and (B) enclosing a luminal structure (confocal z-stack). (C) Flow cytometry analysis (n=3) confirms that EVCs cultured in HA hydrogel culture media for three days acquire NG2 expression. Images shown are typical of the independent experiment. Inset is isotype control. Scale bar is 20µm.

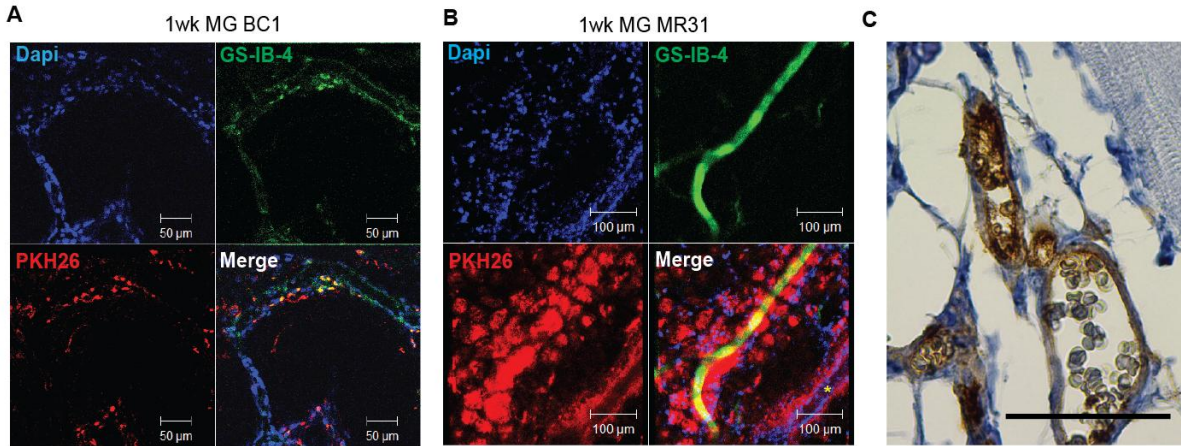


Fig. S14. *In vivo* functionality of EVCs. EVCs derived from (A) BC1 and (B) MR31 were dyed with PKH-26 (non-specific cell red dye), implanted subcutaneously in Matrigel (MG) plugs and explants were analyzed after one week. Prior to sacrifice, mice were tail-vein injected with mouse specific fluorescein-conjugated *GS-IB-4* lectin. Representative confocal z-stack images of perfused explants with mouse specific fluorescein-conjugated *GS-IB-4* lectin (green) show that EVCs integrated into host vasculature after one week (human cells in red). Some human vessels were lacking red blood cells (asterisk). Nuclei in blue. **c**, Histological examination of BC1-MG explants after 1 week reveals functional microvasculature containing human CD31+ cells (brown; counterstain in blue) as indicated by blood cell perfusion. Scale bar is 50 μ m.

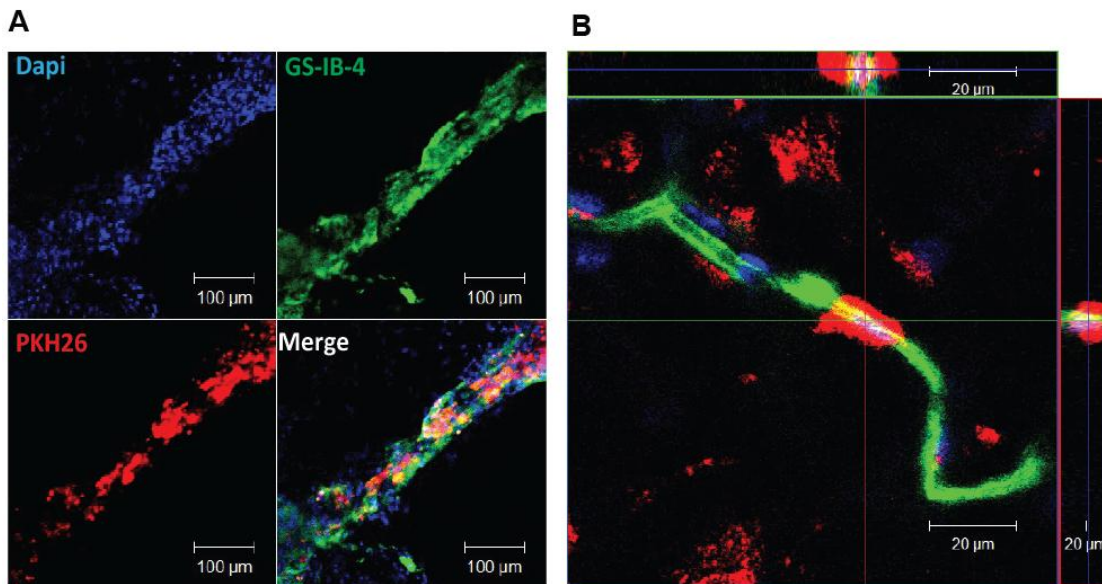


Fig. S15. EC and pericyte phenotypes in *in vivo* explants of BC1-EVC HA constructs. EVCs derived from BC1 were dyed with PKH-26 (non-specific cell red dye), encapsulated in HA hydrogels, and cultured for 3 days, after which were implanted subcutaneously. Prior to sacrifice, mice were tail-vein injected with mouse specific fluorescein-conjugated *GS-IB-4* lectin. Confocal z-stack images of two week explants perfused with fluorescein-conjugated *GS-IB-4* lectin (green) showing human cells (red) interacting with the host vessels (green) via (A) incorporation into and (B) wrapping around penetrating host vessels.

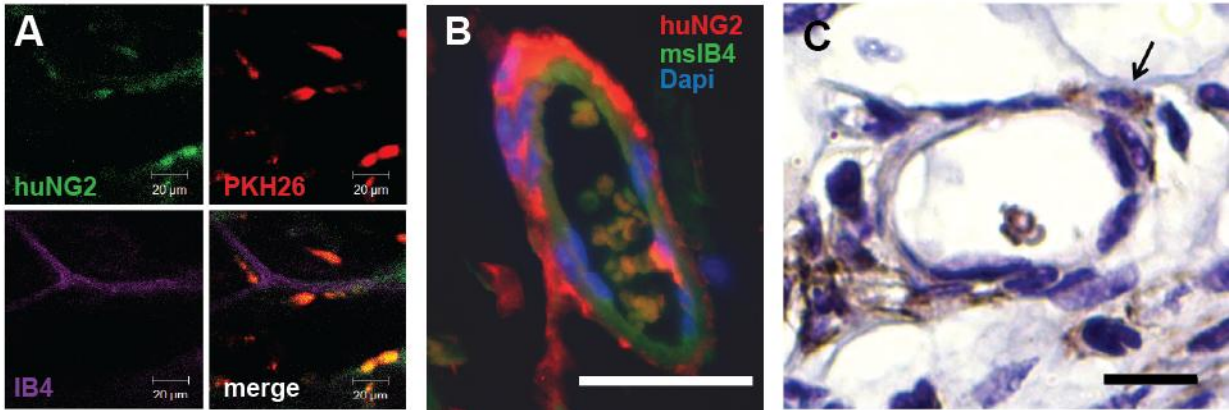


Fig. S16. Derived pericytes *in vivo*. (A) Confocal images of two week explants of BC1-EVC networks in HA hydrogels reveals functional human NG2⁺ (green; human specific antibody) pericytes proximal to host vessels (purple) in two week explants. Human cells are in red (PKH26). (B-C) Histological examination of *in vivo* explants of hESC-H9-EVC networks in HA hydrogels after two weeks also depict NG2⁺ human pericytes wrapping perfused vessels via (B) immunofluorescence staining on cross sections of explants. Scale bar is 20 μm, and (C) immunohistochemistry for human NG2 (in brown; an example is indicated by arrow). Scale bar is 10 μm.

Supplementary Table S1:

hPSC line	Type	Reprogramming factors	Source	Ref.
H9	hESC	--	blastocyst	(17)
MR31	hiPSC	OSK	IMR90 (normal, fetal lung fibroblasts, XX)	(1)
BC1	hiPSC	Plasmid encoding OSKML	CD34+ cells from bone marrow	(2-3)
GFP-hiPSC	hiPSC	OSLN	Cord blood-derived ECs	(4)

hPSC lines studied. O=OCT4; S=SOX2; K=KLF4; M=c-MYC; L=LIN28; N=NANOG

Supplementary Table S2:

Antibody	Source	Catalog #	Purpose	Host Species & Reactivity	Concentration
AcLDL	Invitrogen	L-3484	IF	ECs	10 µg/ml
AlexaFluor 488	Invitrogen	A11008	IF	Goat anti-rabbit	1:1,000
Calponin	Dako	M3556	IF	Mouse anti-human	1:100
CD105-PE	eBioscience	12-1057-41	FC	Mouse anti-human	1:10
CD146-PE	BD	550315	FC	Mouse anti-human	1:10
CD31	Dako	M0823, clone JC70/A	IF; IHC	Mouse anti-human	1:200; 1:50
CD31-PE	BD	555446	FC	Mouse anti-human	1:10
CD44-PE	BD	550989	FC	Mouse anti-human	1:10
CD45-PE	BD	555483	FC	Mouse anti-human	1:10
CD73-PE	eBioscience	12-0739-41 Clone AD2	FC	Mouse anti-human	1:10
Cy3	Sigma	C2181-1ML	IF	Sheep anti-mouse	1:50
Dapi	Roche	10236276	IF	Nucleus	1:1,000
eNOS	BD	610297	IF	Mouse anti-human	1:100
FITC	Sigma	F2883	IF	Sheep anti-mouse	1:50
IgG-Alexa Fluor 488	eBioscience	53-4724-80 Clone eMB2a	FC	Mouse IgG Isotype control	1:10
IgG-FITC	BD	554679	FC	Mouse IgG Isotype Control	1:10
IgG-PE	BD	555749	FC	Mouse IgG Isotype Control	1:10
HRP-secondary	Dako	K4063	IHC	HRP polymer anti-mouse	1:1
NG2	Santa Cruz	sc-53389	IF; IHC	Mouse anti-human	1:100
NG2-Alexa Fluor 488	eBioscience	53-6504-82 Clone 9.2.27	FC; IF	Mouse anti-human	1:10; 1:100
PDGFR β	Santa Cruz	SC-432	IF	Rabbit anti-human	1:100
PDGFR β -PE	R&D	FAB1263P	FC	Mouse anti-human	1:10
Tra-1-60-FITC	BD	560380	FC	Mouse anti-human	1:10
Tra-1-81-FITC	BD	560194	FC	Mouse anti-human	1:10
Ulex lectin	Vector Lab	FL-1061	IF	Human ECs	1:50
VEcad	Santa Cruz	sc-9989	IF	Mouse anti-human	1:200
VEcad-FITC	BD	560411	FC	Mouse anti-human	1:10
VEcad-PE	BD	560410	FC	Mouse anti-human	1:10
VEGFR2-PE	BD	560494	FC	Mouse anti-human	1:10
vWF	Dako	M0616 Clone F8/86	IF	Mouse anti-human	1:200

Antibodies used in the study. IF= immunofluorescence; FC= flow cytometry; IHC= immunohistochemistry

Supplemental References:

1. Mali P, *et al.* (2010) Butyrate greatly enhances derivation of human induced pluripotent stem cells by promoting epigenetic remodeling and the expression of pluripotency-associated genes. *Stem Cells* 28(4):713-720.
2. Chou BK, *et al.* (2011) Efficient human iPS cell derivation by a non-integrating plasmid from blood cells with unique epigenetic and gene expression signatures. *Cell Research* 21(3):518-529.
3. Cheng L, *et al.* (2012) Low Incidence of DNA Sequence Variation in Human Induced Pluripotent Stem Cells Generated by Nonintegrating Plasmid Expression. *Cell Stem Cell* 10(3):337-344.
4. Haase A, *et al.* (2009) Generation of Induced Pluripotent Stem Cells from Human Cord Blood. *Cell Stem Cell* 5(4):434-441.
5. Vo E, Hanjaya-Putra D, Zha Y, Kusuma S, & Gerecht S (2010) Smooth-Muscle-Like Cells Derived from Human Embryonic Stem Cells Support and Augment Cord-Like Structures In Vitro. *Stem Cell Reviews and Reports* 6(2):237-247.
6. Wanjare M, Kuo F, & Gerecht S (2012) Derivation and maturation of synthetic and contractile vascular smooth muscle cells from human pluripotent stem cells. *Cardiovascular Research*.
7. Kusuma S, Zhao S, & Gerecht S (2012) The extracellular matrix is a novel attribute of endothelial progenitors and of hypoxic mature endothelial cells. *FASEB Journal* 26(12):4925-4936.
8. Dickinson LE, Moura ME, & Gerecht S (2010) Guiding endothelial progenitor cell tube formation using patterned fibronectin surfaces. *Soft Matter* 6(20):5109-5119.
9. Orledge A & D'Amore PA (1987) Inhibition of capillary endothelial cell growth by pericytes and smooth muscle cells. *The Journal of Cell Biology* 105(3):1455-1462.
10. Pittenger MF, *et al.* (1999) Multilineage potential of adult human mesenchymal stem cells. *Science* 284(5411):143-147.
11. Grayson WL, *et al.* (2010) Engineering anatomically shaped human bone grafts. *Proceedings of the National Academy of Sciences of the United States of America* 107(8):3299-3304.
12. Khetan S, Katz JS, & Burdick JA (2009) Sequential crosslinking to control cellular spreading in 3-dimensional hydrogels. *Soft Matter* 5(8):1601-1606.
13. S. K & J.A B (2010) Patterning network structure to spatially control cellular remodeling and stem cell fate within 3-dimensional hydrogels. *Biomaterials* 31:8228.
14. Kang K-T, Allen P, & Bischoff J (2011) Bioengineered human vascular networks transplanted into secondary mice reconnect with the host vasculature and re-establish perfusion. *Blood*.
15. Hanjaya-Putra D, *et al.* (2011) Controlled activation of morphogenesis to generate a functional human microvasculature in a synthetic matrix. *Blood* 118(3):804-815.
16. Mead LE, Prater D, Yoder MC, & Ingram DA (2007) Isolation and Characterization of Endothelial Progenitor Cells from Human Blood. *Current Protocols in Stem Cell Biology*, (John Wiley & Sons, Inc.).
17. Thomson JA (1998) Embryonic stem cell lines derived from human blastocysts. *Science* 282(5391):1145-1147.